# Fragmentation Pathways in a Series of $CH_3COX$ Molecules in the Strong Field Regime†

**Smriti Anand, Muhannad M. Zamari, Getahun Menkir, Robert J. Levis, and H. Bernhard Schlegel***

*Department of Chemistry, Wayne State University, Detroit, Michigan 48202, and Department of Chemistry, Temple University, Philadelphia, Pennsylvania 19122*

*Received: October 30, 2003; In Final Form: February 2, 2004*

In intense laser fields, fragment ions can be produced from $CH_3COX$ (X = $CH_3$, $CF_3$, and $C_6H_5$) either by absorption and dissociation followed by ionization (ADI) or absorption and ionization followed by dissociation (AID). Electronic structure calculations were carried out using Hartree−Fock, density functional, and correlated levels of theory to understand the possible fragmentation pathways. The calculated ionization potentials are in very good agreement with the available experimental data. For acetone, the acetyl ion is predicted to be the most preferred dissociation product and can be produced by either mechanism. The very low $C-CF_3$ bond energy in the parent ion of trifluoroacetone provides a clear reason for the absence of $CF_3COCH_3^+$ and $CF_3CO^+$ ion peaks from the mass spectrum of $CF_3COCH_3$ after intense laser excitation and indicates that fragmentation occurs by AID. For acetophenone, both $CH_3CO^+$ and $C_6H_5CO^+$ are stable fragments, with the latter being produced by an AID mechanism.

## Introduction

Strong field chemical investigations have typically focused on the interaction of molecules with 800 nm laser pulses in the intensity regime of $\sim 10^{13}-10^{14}$ W cm$^{-2}$. In this intensity range, the associated magnitude of the electric field of the radiation is on the order of the binding energy of the valence electrons in a molecule.[1,2] All molecules that have been probed to date provide ion signals, often with the parent ion detected in addition to a variety of fragment ions. Recent experiments demonstrated that the yield of dissociative ionization channels can be controlled using shaped laser pulses in the strong field regime. In particular, the product yield distributions for a series of $CH_3COX$ molecules (where X = $CH_3$, $CF_3$, and $C_6H_5$) have been manipulated by using closed-loop methods[3] to determine the optimal pulse shape for a pre-specified reaction channel. Varying the phase and amplitude of the control pulse induced the selective cleavage and rearrangement of chemical bonds. Since this experiment was performed in the strong field regime, our understanding of the detailed mechanism of the control is limited.

In some molecules, strong field ionization produces a fragmentation distribution that is very similar to the distribution observed using electron impact ionization.[4] This may be rationalized by a similar impulsive energy deposition mechanism for the two methods, since the interaction time (∼tens of femtoseconds) and interaction energies (∼tens of electronvolts) are comparable. In the present work, we wish to obtain a first-order understanding of the fragmentation distributions of $CH_3COX$ in the impulsive limit. In both strong field ionization and electron impact ionization, the energy is deposited rapidly and the molecule cools by dissociation into fragments. The distribution of products may be determined by the energetic ordering of the product states. Similar to the computational studies in conventional mass spectrometry,[5,6] we would like to see whether the calculated energetics for the dissociation pathways on the field free energy surfaces can explain certain observations in the fragmentation patterns in strong field chemistry. In particular, we wish to understand the absence of $CF_3CO^+$ and $CF_3COCH_3^+$ intensity peaks from the time-of-flight mass spectrum of $CF_3COCH_3$.

## Experimental Methods

The mass spectrometer and laser system have been previously described.[3] The laser produces 50 fs pulses having energies of 1 mJ/pulse at 10 Hz. The maximum intensity produced after focusing the laser to a 100 micrometer spot size in the extraction region of the mass spectrometer is $2 \times 10^{14}$ W cm$^{-2}$. The mass spectrometer used to detect the reaction channels is a linear time-of-flight system with a 1 m drift tube employing a microchannel plate to detect and amplify the ion signal. The gas-phase samples are introduced using a variable leak valve and the pressure is maintained at $10^{-6}$ Torr.

## Computational Methods

Electronic structure calculations were carried out using the Gaussian series of programs.[7] The geometries of the $CH_3COX$ molecule and their fragments (both neutrals and ions) were optimized at the HF/3-21G, B3LYP/6-31G(d), B3LYP/CBSB7, and MP2/6-31G(d) levels of theory as well as QCISD/6-311G(d,p). The ionization potentials (IP) were calculated by taking the difference between the energy of the neutral and the ion (CBS-QB3 calculation[8,9]) and compared to the experimental IP. The energetics of the dissociation of the parent molecules (neutrals and ions) into possible fragments were calculated at the CBS-QB3 level of theory. To explore the potential energy surface, reaction path scans were carried out at the HF/3-21G level before transition states were calculated at the CBS-QB3 level.

## Results and Discussion

The strong field mass spectrum for acetone has been reported previously[3] and displays features corresponding to $CH_3^+$, $CH_3CO^+$, and $(CH_3)_2CO^+$, similar to the electron impact

† Part of the special issue "Fritz Schaefer Festschrift".

* Corresponding author.

10.1021/jp0372789 CCC: $27.50 
Published on Web 03/06/2004

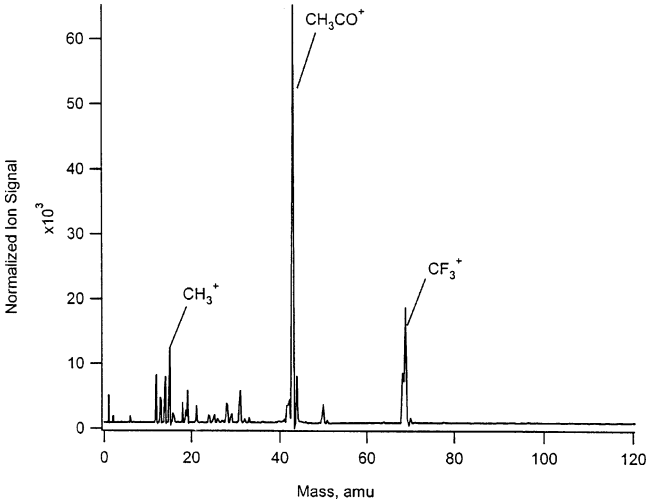


**Figure 1.** Strong field mass spectrum of trifluoroacetone ($CF_3COCH_3$).

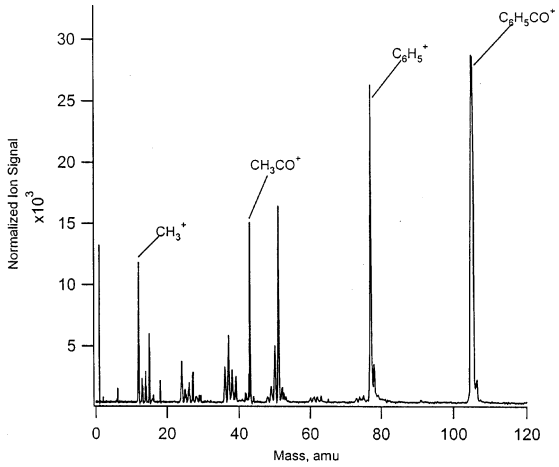


**Figure 2.** Strong field mass spectrum of acetophenone ($C_6H_5COCH_3$).

spectrum.[10] The mass spectra for trifluoroacetone and acetophenone are shown in Figures 1 and 2, respectively. In the case of $CF_3COCH_3$, the mass spectrum reveals features for $CH_3^+$, $CH_3CO^+$, and $CF_3^+$, with the dominant feature being the $CH_3CO^+$ peak. There are no mass spectral features corresponding to the $CF_3CO^+$ and $CF_3COCH_3^+$ ions, in contrast to the electron impact spectrum which does show small peaks for these ions. The mass spectral ion intensity distribution remains largely unchanged even with an order of magnitude reduction in the laser intensity. In acetophenone, the predominant peak corresponds to $C_6H_5CO^+$ (Figure 2). In the transform limited pulse strong field mass spectrum, the parent ion at mass 120 is not visible, as indicated previously,[3] but can be detected with lower intensity pulses (not shown) and can be seen in the electron impact spectra. The parent ion is not stable at higher intensities in the strong field spectrum and dissociates by cleavage of either the methyl group or the phenyl group.

There are two basic scenarios for the production of fragment peaks in any laser-based excitation scheme: absorption and dissociation followed by ionization (ADI); and absorption and ionization of the parent followed by dissociation (AID). To obtain a first-order understanding of the relative importance of these two mechanisms, we consider the energetics of fragmentation of both the neutral and ionized parent molecules. We assume a quasi statistical distribution is produced during energy deposition as a result of the spatial distribution of the large number of molecules interacting with the laser pulse. In the absence of any significant energy barriers, this leads to a fragmentation distribution governed by the energetics of the various product states.

**TABLE 1: Calculated and Experimental Ionization Potential of $CH_3COX$ and Its Fragments**

| molecule | energy[a]/hartrees | IP[b]/eV (calcd) | IP/ eV (expt) |
|---|---|---|---|
| $CH_3COCH_3$ | −192.819611 | | |
| $CH_3COCH_3^{\cdot+}$ | −192.461646 | 9.74 | 9.70[c] |
| $CF_3COCH_3$ | −490.333083 | | |
| $CF_3COCH_3^{\cdot+}$ | −489.94187 | 10.65 | 10.67[d] |
| $C_6H_5COCH_3$ | −384.210425 | | |
| $C_6H_5COCH_3^{\cdot+}$ | −383.868209 | 9.31 | 9.28[e] |
| $CH_3CO^{\cdot}$ | −152.942026 | | |
| $CH_3CO^+$ | −152.685818 | 6.97 | 7.00[f] |
| $CF_3CO^{\cdot}$ | −450.445780 | | |
| $CF_3CO^+$ | −450.129189 | 8.61 | |
| $C_6H_5CO^{\cdot}$ | −344.331452 | | |
| $C_6H_5CO^+$ | −334.093436 | 6.48 | |
| $^{\cdot}CH_3$ | −39.744795 | | |
| $CH_3^+$ | −39.384665 | 9.80 | 9.84[g] |
| $^{\cdot}CF_3$ | −337.254547 | | |
| $CF_3^+$ | −336.919406 | 9.12[b]9.07 [h] | 9.04 [i] |
| $^{\cdot}C_6H_5$ | −231.108297 | | |
| $C_6H_5^+$ | −230.807840 | 8.18 | 8.32[j] 8.1[k] |

[a] CBS-QB3 value. [b] CBS-QB3 value. [c] Ref 17. [d] Ref 18. [e] Ref 19. [f] Ref 20. [g] Ref 21. [h] CBS-APNO value. [i] Ref 22. [j] Ref 23. [k] Ref 24.

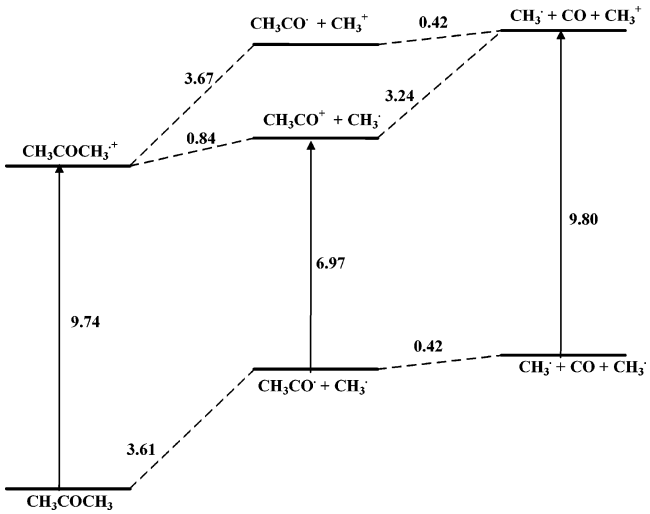


**Figure 3.** Dissociation and ionization pathways for acetone calculated at the CBS-QB3 level of theory (energies in eV).

To validate the level of electronic structure theory used in the calculations, we first computed the adiabatic ionization potentials of acetone, trifluoroacetone, acetophenone, and the fragments. The calculated results are shown in Table 1 along with the experimentally measured values where available. Comparison of the data indicates that the calculated IP's are within about 0.04−0.1 eV of the experimental values. As seen from the table, the calculated IP of trifluoroacetone is higher than acetone (10.65 eV vs 9.74 eV). This can be attributed to the fact that the highly electronegative fluorine atoms have an inductive electron withdrawing effect and hence the presence of the $CF_3$ group makes ionization more difficult. The same effects are responsible for the higher IP of $CF_3CO$ compared to $CH_3CO$. There is no data available on the experimental IP of the trifuoroacetyl ($CF_3CO$) and benzoyl ($C_6H_5CO$) radicals. Since the calculated and experimental IP's of the other fragments are in very good agreement, our calculated IP's for $CF_3CO$ and

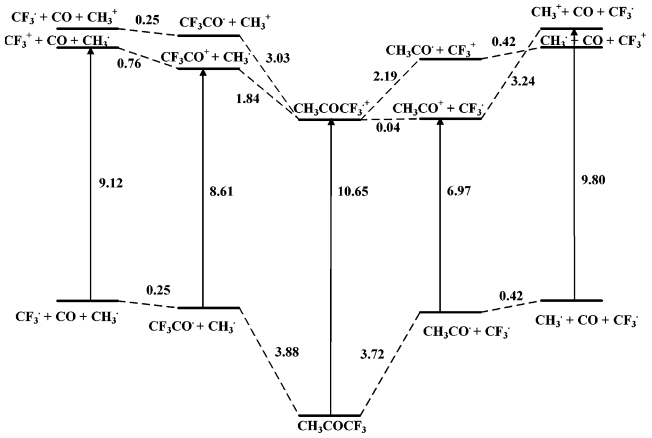


**Figure 4.** Dissociation and ionization pathways for trifluoroacetone calculated at the CBS-QB3 level of theory (energies in eV).

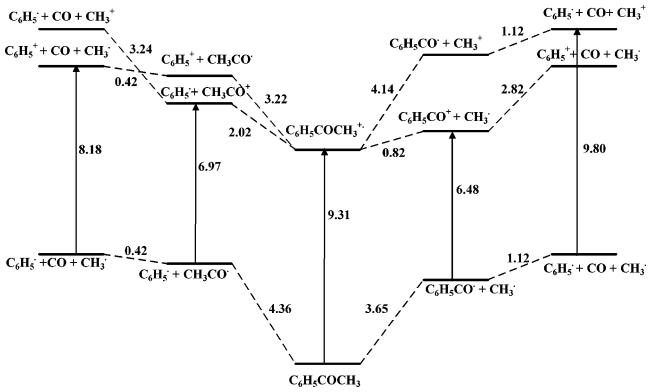


**Figure 5.** Dissociation and ionization pathways for acetophenone calculated at the CBS-QB3 level of theory (energies in eV).

$C_6H_5CO$ should be very good estimates of the actual values. These IP's are necessary to construct the energy diagrams shown in Figures 3−5.

When acetone is ionized, the unpaired electron is found to be located on the oxygen atom and the positive charge is largely on the carbonyl carbon. The possible dissociation pathways for acetone are presented in Figure 3. As can be seen, the energy for the dissociation of acetone cation into $CH_3CO + CH_3^+$ (3.67 eV) is comparable to the formation of $CH_3CO + CH_3$ from neutral acetone (3.61 eV). However, dissociation of $CH_3COCH_3^+$ into $CH_3CO^+ + CH_3$ is much easier (0.84 eV). The acetyl cation ($CH_3CO^+$) is a closed shell molecule stabilized by a triple bond between C and O. This accounts not only for the low dissociation energy for the $CH_3COCH_3^+ \rightarrow CH_3CO^+ + CH_3$ reaction but also for the low IP of $CH_3CO$ (6.97 eV compared to 9.74 eV for acetone). Thus, if one considers the ADI mechanism, one would expect that the acetyl cation would be formed in greater proportion than the other fragments. On the other hand, if the fragmentation followed the AID mechanism, one would again expect the acetyl ion to be formed with ease. This is because the bond dissociation energy in the case of $CH_3COCH_3^+$ forming $CH_3CO^+$ and $CH_3$ (0.84 eV) is much smaller than the applied field. Thus both mechanisms could account for the dominance of the $CH_3CO^+$ in the mass spectrum.

In trifluoroacetone, the $F_3C-C$ bond is found to be longer than the $H_3C-C$ bond in both the neutral and the cation. The unpaired electron in the ion is on the oxygen atom and there is a large positive charge on the carbon atom bearing the fluorine atoms (due to the electronegativity of the fluorine atoms). As seen in Figure 4, the $CF_3-C$ and $CH_3-C$ bond dissociation energies in neutral trifluoroacetone are nearly equal (3.72 and 3.88 eV, respectively) and are very similar to the $C-CH_3$ bond energy in acetone (3.61 eV). The computed energetics for the subsequent dissociation of the acyl radicals, 0.25 eV for $CF_3CO$ and 0.42 eV for $CH_3CO$, are in good agreement with published experimental and calculated dissociation energies[11−14] (but it should be noted that these processes have barriers that are 0.2−0.3 eV above the dissociation energy). Of the possible dissociation paths for $CF_3COCH_3$, formation of $CH_3^+$ and $CF_3^+$ are disfavored because these have higher IP's than $CX_3CO$. Production of $CH_3CO^+$ is preferred thermodynamically because of the stability of acetyl cation. The trifluoroacetyl cation ($CF_3CO^+$) is less stable than $CH_3CO^+$ because of orbital interactions between the fluorine lone pairs and the C−C anti bonding orbital, leading to a much longer C−C bond in $CF_3CO^+$ than in $CH_3CO^+$ (1.69 Å vs 1.45 Å, respectively). These same interactions are responsible for the difference between the $CF_3-C$ and $CH_3-C$ bond lengths calculated for $CF_3COCH_3^+$ (1.94 Å vs 1.48 Å, respectively). These orbital interactions also account for the low C−C bond dissociation energy in $CF_3CO^+$ (0.76 eV vs 3.24 eV in $CH_3CO^+$). Thus $CH_3CO^+$ should be the most abundant fragment ion formed from the ionization of trifluoroacetone, since it requires the least energy to be produced and is the most stable toward further dissociation. This is in

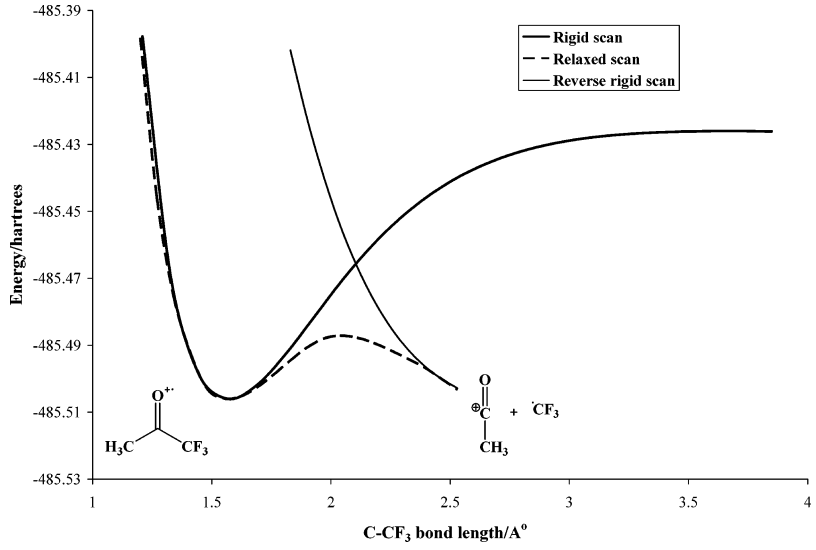


**Figure 6.** Potential energy scan along the $C-CF_3$ bond in trifluoroacetone at the HF/3-21G level of theory.

agreement with the strong field mass spectrum, Figure 1, as well as the electron impact mass spectrum.

The $CF_3-C$ bond in trifluoroacetone cation shows significant elongation and a very low dissociation energy (0.04 eV) for that bond. A relaxed potential energy surface scan along this bond revealed the presence of a barrier (Figure 6). This can be understood in terms of an avoided crossing between the potentials for the valence bond structures representing the reactants and the products. The behavior of these curves can be approximated by rigid scans from the reactant and product sides, as illustrated in Figure 6. At the CBS-QB3 level, the transition state resides only 0.027 eV above the trifluoroacetone cation. This can be compared with 0.84 eV for $CH_3-C$ dissociation in $CH_3COCH_3^+$, and dissociation occurs with little or no barrier above the thermodynamic dissociation energy. In the case of $CF_3COCH_3$, no mass spectral features corresponding to $CF_3CO^+$ and $CF_3COCH_3^+$ were detected and the dominant peak is the $CH_3CO^+$ fragment. We therefore turn our attention to the energetics of the $C-CF_3$ bond in $CF_3COCH_3^+$ as a possible explanation for the absence of these peaks. The low energy for the $C-CF_3$ bond dissociation in $CF_3COCH_3^+$ (0.04 eV) suggests that once the parent ion is formed, dissociation into $CH_3CO^+$ and $CF_3$ is inescapable. This fact explains the absence of $CF_3COCH_3^+$ and $CF_3CO^+$ intensity peaks from the mass spectrum of $CF_3COCH_3$. By contrast, the bond dissociation energy in acetone is higher and not all parent ions undergo dissociation as in trifluoroacetone. This suggests that the most important dissociation mechanism during the radiation-$CF_3COCH_3$ coupling is AID.

In the acetophenone radical cation, the spin due to the unpaired electron is found to be delocalized on to the $\pi$ system of the phenyl ring. The positive charge is greatest on the carbon atom in the ring to which the acetyl group is attached. In the neutral acetophenone, the carbonyl group (C═O) is in the same plane as the benzene ring. However, in the ion, the C═O group makes an angle of 42° with the benzene ring. The $CH_3-C$ and $C_6H_5-C$ bond dissociation energies in acetophenone are 3.65 and 4.36 eV respectively (see Figure 5). These dissociation energies as well as the $C_6H_5-C$ bond energy in $C_6H_5CO$ (1.12 eV) are in very good agreement with experiment.[15,16] The dissociation of the $CH_3-C$ bond in acetophenone is very similar to the dissociation energies in both acetone (3.61 eV) and trifluoroacetone (3.88 eV), while conjugation contributes to the higher $C_6H_5-C$ bond energy. The IP of acetophenone (9.31 eV) is lower than acetone and trifluoroacetone because of the delocalization of the unpaired electron in the benzene ring. Direct formation of $CH_3^+$ and $C_6H_5^+$ is disfavored because these have higher IP's than either $C_6H_5CO$ (benzoyl) or $CH_3CO$ (acetyl) (6.48 and 6.97 eV, respectively). Production of $C_6H_5CO^+$ is preferred thermodynamically because of stabilization due to $\pi$-cloud delocalization. This delocalization is also responsible for the low IP for $C_6H_5$ (8.18 eV) as compared to $CH_3$ (9.80 eV). The high stability of the $C_6H_5CO^+$ fragment accounts for the low bond dissociation energy of the $C-CH_3$ bond in $C_6H_5COCH_3^+$ (0.82 eV vs 2.02 eV for the $C_6H_5-C$ bond). Thus, in the mass spectrum, one would expect the benzoyl and acetyl cations to be the dominant fragments via AID mechanism. Phenyl cation can be formed by the subsequent dissociation of $C_6H_5CO^+$ as well as by direct dissociation of $C_6H_5COCH_3^+$.

## Conclusions

We have presented an investigation of the possible ionization/dissociation processes for a series of $CH_3COX$ molecules. From the calculated bond dissociation energies, we are able to anticipate the dissociation pathways and thus explain the ion intensities observed in the strong field spectrum. In acetone, both the AID and ADI mechanisms could be responsible for the dominance of the acetyl ion in the strong field mass spectrum. In trifluoroacetone, both the ADI and AID mechanisms are able to explain the absence of the $CF_3CO$ peak in the spectrum. However, the bond energetics suggests that the AID mechanism may be the dominant process during the dissociation of $CF_3COCH_3$. In acetophenone cation, the dissociation of the $C-CH_3$ bond is facile due to the high stability of the benzoyl radical. We predict the benzoyl and acetyl cations to be major fragments with the AID mechanism dominating the formation of the benzoyl cation.

**Acknowledgment.** This work was supported by the Department of Defense MURI program as managed by the Army Research Office (R.J.L.) and grants from the National Science Foundation (CHE 0131157 to H.B.S., CHE 0213483 to R.J.L.). The authors thank the National Center for Supercomputing Applications and ISC at WSU for computer time.

## References and Notes

(1) Levis, R. J.; DeWitt, M. J. *J. Phys. Chem. A* **1999**, *103*, 6493.
(2) Levis, R. J.; Rabitz, H. A. *J. Phys. Chem. A* **2002**, *106*, 6427.
(3) Levis, R. J.; Menkir, G. M.; Rabitz, H. *Science* **2001**, *292*, 709.
(4) Billotto, R.; Levis, R. J. *J. Phys. Chem. A* **1999**, *103*, 8160.
(5) Alcami, M.; Mo, O.; Yanez, M. *Mass Spectrom. Rev.* **2001**, *20*, 195.
(6) Lifshitz, C. *Chem. Soc. Rev.* **2001**, *30*, 186.
(7) Frisch, M. J.; Trucks, G. W.; Schlegel, H. B.; Scuseria, G. E.; Robb, M. A.; Cheeseman, J. R.; Montgomery, J. A.; Vreven, T.; Kudin, K. N.; Burant, J. C.; Millam, J. M.; Iyengar, S.; Tomasi, J.; Barone, V.; Mennucci, B.; Cossi, M.; Scalmani, G.; Rega, N.; Petersson, G. A.; Nakatsuji, H.; Hada, M.; Ehara, M.; Toyota, K.; Fukuda, R.; Hasegawa, J.; Ishida, M.; Nakajima, T.; Honda, Y.; Kitao, O.; Nakai, H.; Klene, M.; Li, X.; Knox, J. E.; Hratchian, H. P.; Cross, J. B.; Adamo, C.; Jaramillo, J.; Gomperts, R.; Stratmann, R. E.; Yazyev, O.; Austin, A. J.; Cammi, R.; Pomelli, C.; Ochterski, J.; Ayala, P. Y.; Morokuma, K.; Voth, G. A.; Salvador, P.; Dannenberg, J. J.; Zakrzewski, V. G.; Dapprich, S.; Daniels, A. D.; Strain, M. C.; Farkas, O.; Malick, D. K.; Rabuck, A. D.; Raghavachari, K.; Foresman, J. B.; Ortiz, J. V.; Cui, Q.; Baboul, A. G.; Clifford, S.; Cioslowski, J.; Stefanov, B. B.; Liu, G.; Liashenko, A.; Piskorz, P.; Komaromi, I.; Martin, R. L.; Fox, D. J.; Keith, T.; Al-Laham, M. A.; Peng, C. Y.; Nanayakkara, A.; Challacombe, M.; Gill, P. M. W.; Johnson, B.; Chen, W.; Wong, M. W.; Andres, J. L.; Gonzalez, C.; Replogle, E. S.; Pople, J. A. Gaussian 03 rev. A1; Gaussian, Inc.: Pittsburgh, PA, 2003.
(8) Montgomery, J. A.; Ochterski, J. W.; Petersson, G. A. *J. Chem. Phys.* **1994**, *101*, 5900.
(9) Montgomery, J. A.; Frisch, M. J.; Ochterski, J. W.; Petersson, G. A. *J. Chem. Phys.* **1999**, *110*, 2822.
(10) *NIST Chemistry WebBook*; Linstrom, P. J., Mallard, W. G., Eds.; National Institute of Standards and Technology: Gaithersburg, MD, 2001.
(11) Maricq, M. M.; Szente, J. J.; Khitrov, G. A.; Dibble, T. S.; Francisco, J. S. *J. Phys. Chem.* **1995**, *99*, 11875.
(12) Tomas, A.; Caralp, F.; Lesclaux, R. *Z. Phys. Chem.* **2000**, *214*, 1349.
(13) Viskolcz, B.; Berces, T. *Phys. Chem. Chem. Phys.* **2000**, *2*, 5430.
(14) Mereau, R.; Rayez, M. T.; Rayez, J. C.; Caralp, F.; Lesclaux, R. *Phys. Chem. Chem. Phys.* **2001**, *3*, 4712.
(15) Zhao, H. Q.; Cheung, Y. S.; Liao, C. L.; Liao, C. X.; Ng, C. Y.; Li, W. K. *J. Chem. Phys.* **1997**, *107*, 7230.
(16) Nam, G. J.; Xia, W. S.; Park, J.; Lin, M. C. *J. Phys. Chem. A* **2000**, *104*, 1233.
(17) Traeger, J. C.; McLoughlin, R. G.; Nicholson, A. J. C. *J. Am. Chem. Soc.* **1982**, *104*, 5318.
(18) Cocksey, B. J.; Eland, J. H. D.; Danby, C. J. *J. Chem. Soc.* **1971**, *(B)*, 790.
(19) McLoughlin, R. G.; Traeger, J. C. *Org. Mass Spectrom.* **1979**, *14*, 434.
(20) Lias, S. G.; Bartmess, J. E.; Liebman, J. F.; Holmes, J. L.; Levin, R. D.; Mallard, W. G. *J. Phys. Chem. Ref. Data* **1988**, *17*, 1.
(21) Berkowitz, J.; Ellison, G. B.; Gutman, D. *J. Phys. Chem.* **1994**, *98*, 2744.
(22) Garcia, G. A.; Guyon, P. M.; Powis, I. *J. Phys. Chem. A* **2001**, *105*, 8296.
(23) Butcher, V.; Costa, M. L.; Dyke, J. M.; Ellis, A. R.; Morris, A. *Chem. Phys.* **1987**, *115*, 261.
(24) Sergeev, Y. L.; Akopyan, M. E.; Vilesov, F. I. *Opt. Spectrosc.* **1972**, *32*, 121.